

## Transparent and conductive paper from nanocellulose fiberst

Cite this: *Energy Environ. Sci.*, 2013, **6**, 513

Liangbing Hu,<sup>†a</sup> Guangyuan Zheng,<sup>‡b</sup> Jie Yao,<sup>a</sup> Nian Liu,<sup>c</sup> Ben Weil,<sup>a</sup> Martin Eskilsson,<sup>d</sup> Erdem Karabulut,<sup>d</sup> Zhichao Ruan,<sup>e</sup> Shanhui Fan,<sup>e</sup> Jason T. Bloking,<sup>a</sup> Michael D. McGehee,<sup>a</sup> Lars Wågberg<sup>\*d</sup> and Yi Cui<sup>\*af</sup>

Here we report on a novel substrate, nanopaper, made of cellulose nanofibrils, an earth abundant material. Compared with regular paper substrates, nanopaper shows superior optical properties. We have carried out the first study on the optical properties of nanopaper substrates. Since the size of the nanofibrils is much less than the wavelength of visible light, nanopaper is highly transparent with large light scattering in the forward direction. Successful depositions of transparent and conductive materials including tin-doped indium oxide, carbon nanotubes and silver nanowires have been achieved on nanopaper substrates, opening up a wide range of applications in optoelectronics such as displays, touch screens and interactive paper. We have also successfully demonstrated an organic solar cell on the novel substrate.

Received 27th September 2012  
Accepted 19th November 2012

DOI: 10.1039/c2ee23635d

[www.rsc.org/ees](http://www.rsc.org/ees)

### Broader context

Wood fiber cellulose has been used for more than 2000 years as an ingredient for making paper. The cellulose paper that we see in our everyday lives consists of fibers with diameters of tens of micrometers. Using chemical or enzymatic pretreatments followed by high-pressure homogenization, the micrometer-sized cellulose fibers can be disintegrated into nanofibrillated cellulose (NFC) with a diameter of around 10–20 nm and a length of 2  $\mu\text{m}$ . By compressing the NFC pulp with the right composition in a sheet-former, highly transparent nanocellulose paper can be produced. The nanocellulose paper has large light scattering in the forward direction, which is very useful for solar cell applications. The nanocellulose paper can be coated with a wide variety of conductive materials, such as carbon nanotubes, silver nanowires and tin-doped indium oxide (ITO), to produce transparent conductive paper. By depositing a thin layer of ITO, the conductive nanocellulose paper can be used as a substrate for making organic solar cells.

### Introduction

Cellulose is the most abundant organic material on earth and a key source of many types of sustainable materials. Paper, a widely used material in everyday life, is a product made of cellulose that has been used ubiquitously and has an ancient history. It is a low cost, flexible and porous substrate that allows for fast printing and strong binding of other materials. Recently, paper has been explored for electronics and power

applications. Thin film transistors, solar cells and batteries have all been demonstrated using paper as a substrate.<sup>1–3</sup> Often, the porous structure of paper not only simplifies the fabrication process towards low cost techniques, but also enhances the device performance by providing additional structural advantages to manipulate electrons, ions and photons.<sup>1,4,5</sup> However, since paper is made of cellulose fibers with diameters of  $\sim 20 \mu\text{m}$ , there are intrinsic disadvantages regarding emerging applications. Paper is usually extremely rough, with peak-to-valley roughness values of up to hundreds of micrometers. Since the fiber diameter is much larger than the wavelength of visible light, paper is usually not transparent. The packing density of fibers also limits its overall mechanical properties. These disadvantages of paper limit its applications in certain areas, including the emerging field of printed electronics. Meanwhile, a paper fiber with  $\sim 20 \mu\text{m}$  diameter is made of millions of cellulose nanofibrils with a cross-sectional diameter of  $\sim 4 \text{ nm}$  and a length of  $\sim 2 \text{ mm}$ . Another way to make a paper sheet is to disintegrate these cellulose nanofibrils in solution, using a high pressure homogenizer, and reform them in such a way that the solvent is filtered through a commercial membrane. Such new paper made of cellulose nanofibrils is

<sup>a</sup>Department of Materials Science and Engineering, Stanford University, Stanford, California 94305, USA. E-mail: [yicui@stanford.edu](mailto:yicui@stanford.edu)

<sup>b</sup>Department of Chemical Engineering, Stanford University, Stanford, California 94305, USA

<sup>c</sup>Department of Chemistry, Stanford University, Stanford, California 94305, USA

<sup>d</sup>Fibre and Polymer Technology, KTH Royal Institute of Technology, Teknikringen 56, 10044 Stockholm, Sweden. E-mail: [wagberg@kth.se](mailto:wagberg@kth.se)

<sup>e</sup>Department of Applied Physics, Stanford University, Stanford, California 94305, USA

<sup>f</sup>Stanford Institute for Materials and Energy Sciences, SLAC National Accelerator Laboratory, 2575 Sand Hill Road, Menlo Park, California 94025, USA

<sup>†</sup> Electronic supplementary information (ESI) available. See DOI: 10.1039/c2ee23635d

<sup>‡</sup> These authors contributed equally to this work.

called nanopaper in this work. This concept has been demonstrated recently.<sup>6–10</sup> Such nanopaper solves the above-mentioned problems of regular paper by providing excellent mechanical properties, optical transparency and a smooth surface (Fig. S1†). These properties will enable a range of applications of paper-based electronics. In this work, we use a scalable process to make transparent and conductive nanopaper. In particular, the large difference between diffusive and specular transmittance is promising for solar cell applications. Such transparent substrates with fibrous structures allow for easy printing and they are attractive replacements for plastic substrates in large-scale flexible electronics and optoelectronic devices.<sup>11,12</sup>

## Main text

Fig. 1 illustrates the fundamental optical properties of transparent nanopaper. A random network of hundreds of nanofibrillated cellulose (NFC) fibrils forms a highly porous structure. As the diameter of the NFC is in the range of  $\sim 4$  nm, the light scattering effect is significantly reduced compared with regular paper. The light scattering of a single NFC fiber scales with the fiber diameter as proportional to  $\sim D$ .<sup>3,13</sup> As the fiber diameter decreases from  $20\ \mu\text{m}$  to  $4$  nm, the back-scattering effect is largely decreased. Each individual nanofiber will lead to small forward scattering. Even when nanopaper is made of hundreds of layers of these 1D nanostructures, most of the light still propagates through the nanopaper. The result is a highly transparent substrate with large scattering in the forward direction. This is the major difference between paper and plastic substrates, which may enable some new applications and opportunities.

To fabricate nanopaper, carboxymethylated NFC was prepared by disintegrating the softwood cellulose fiber in a high-pressure homogenizer according to a procedure described by Wågberg *et al.*<sup>14</sup> Typically, a gel with 2 wt% of the carboxymethylated cellulose in water was obtained (Fig. 2a). The diameter of the NFC was studied with atomic force microscopy (AFM). The diameter of the NFC fiber is found to be  $10$  nm and the length is  $\sim 2\ \mu\text{m}$  (Fig. 2b). A semi-automatic paper sheet-former equipped with draining and compression drying units was used to prepare the NFC paper sheets.  $70$  g of 2 wt% NFC gel

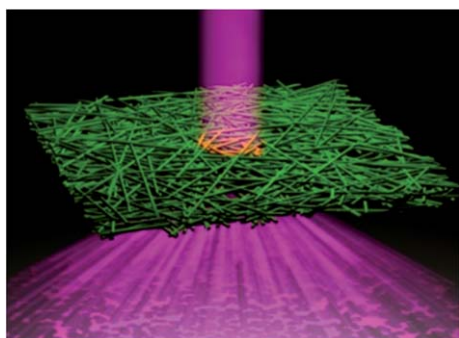


Fig. 1 Schematic of nanocellulose paper and its light scattering effect.

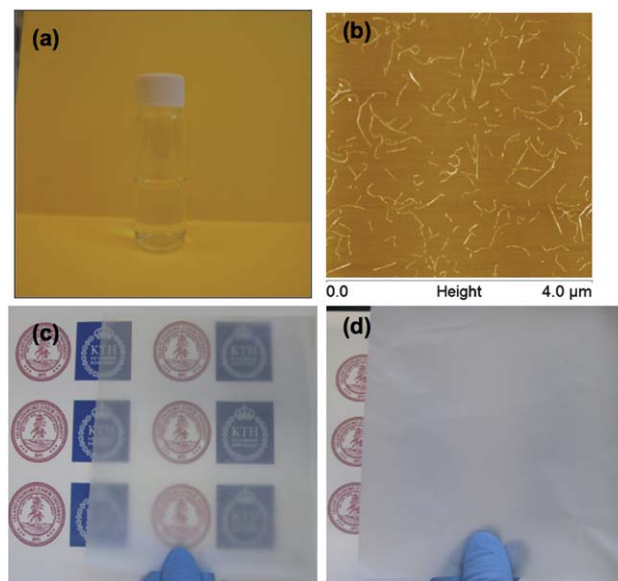
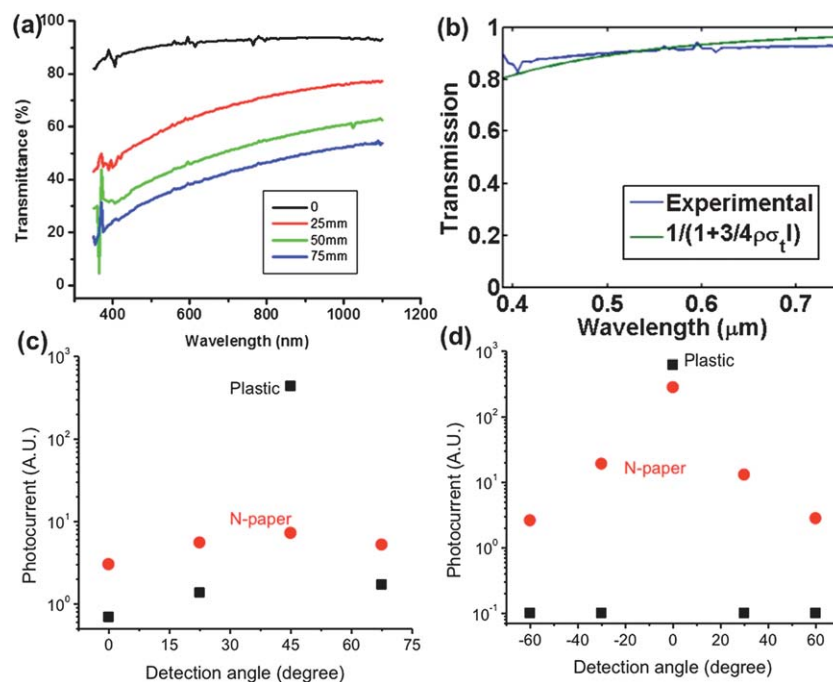


Fig. 2 Transparent paper prepared from nanocellulose dispersion. (a) A picture of the NFC dispersion in water with a concentration of  $1.4\ \text{g L}^{-1}$ . (b) AFM height image of cellulose nanofibrils on a mica substrate. (c) Transparent nanocellulose paper with close contact to the images underneath to indicate its high optical transparency. (d) The same nanocellulose paper at a distance of 2 inches from the images underneath to indicate its large light scattering effect.

was diluted by adding  $200$  mL of water and the dispersion was homogenized for 20 minutes at  $13\ 500$  rpm using a homogenizer. The dispersion was degassed in a sonication bath for 10 minutes and  $500$  mL of water was added under constant stirring. A nitrocellulose ester filter membrane with  $0.65$  mm pore size was placed onto a metal sieve and the viscous dispersion was poured into the draining chamber of the paper sheet-former. The excess water was removed until a smooth, gel-like cake was obtained. The gel was peeled off from the filter membrane and sandwiched between pieces of metal wire cloth. This set-up was sandwiched between two paper carrier boards and was placed into the drying unit of the paper sheet-former where the temperature and pressure were adjusted to  $70\ ^\circ\text{C}$  and  $1$  bar, respectively. The typical nanopaper thickness is  $\sim 40\ \mu\text{m}$ . The nanopaper is highly transparent when it is placed close to the substrate (Fig. 2c). When the nanopaper is around 2 inches away from the substrate, it is hazy and the substrate cannot be observed clearly (Fig. 2d).

The optical properties of nanopaper were compared with a polyethylene terephthalate (PET) plastic substrate. The first set of experiments were on their optical transmittance when the light detector was placed at different distances from the substrate. The beam size was  $5$  mm and the size of the detector was  $1$  cm. As the detector moved away from the substrate, the fraction of the light collected shows the divergence of the transmitted light. The distance between the substrate and the collector was set as  $0$  mm,  $25$  mm,  $50$  mm and  $75$  mm. There was a striking difference between the optical transmittances of nanopaper and that of the plastic substrate (Fig. 3a). As the detector moved away, the transmittance for the PET substrate did not change, but it changed dramatically for nanopaper. This



**Fig. 3** Optical properties of nanopaper. (a) Spectral transmittance of transparent nanopaper. The distance refers to the distance between the detector and the nanopaper. (b) Optical modeling of the spectral transmittance of nanopaper. (c) Angular reflection comparison for plastic substrate and nanopaper. (d) Angular transmittance comparison for plastic substrate and nanopaper.

difference between the nanopaper and plastic substrates can be understood conceptually. Plastic is composed of a dense structure, which is highly uniform on a large scale (comparable or larger than wavelength of light). Therefore, no light scattering is observed.

Since the nanopaper is made of 1D nanostructures with high porosity, the material has large-scale non-uniformity, leading to the observation of light scattering. However, as the basic building block size reduced from microns to a few nanometers, the amount of light scattered became small and was mainly in the forward direction, which is a significant improvement compared to conventional paper. Larger fibers will significantly increase back scattering, so do bigger pore sizes. By reducing the cellulose fibers to nanofibrils of a few nanometers in diameter, back scattering is attenuated. At the same time, the close packing of nanofibrils creates a dense film, which also helps in reducing the scattering of light. Optical modeling with a random medium model was carried out to further investigate this phenomenon. Since an NFC fiber is much smaller than the wavelength of light, the scattering of a single NFC fibril is isotropic, *i.e.* the scattering in the forward and backward directions is equal. The large transmission is dependent upon the small total scattering. The transition through a random-medium slab can be modeled by a theory derived from the Chandrasekhar radiative-transfer equation, with

$$T = \frac{1}{1 + \frac{3}{4}\rho\sigma_{\text{sc}}h}$$

absorption, where  $\rho$  is the density,  $\sigma_{\text{sc}}$  is the scattering cross-section of a single scatter object, and  $h$  is the thickness of the slab.<sup>15</sup> For nanopaper consisting of random NFC fibrils, the

scattering cross-section of a single NFC fibril is the averaged value for different polarizations, different incident angles, and different radii. Using the Mie method,<sup>16</sup> we calculate the scattering cross-section, assuming that the refractive index of the NFC fibers is 1.8 and their diameters are uniform at 4 nm. Fig. 3b shows the comparison between the calculation and the experimental data. Here the parameters for  $h$  and  $\rho$  were set at 40 μm and  $4 \times 10^4 \mu\text{m}^{-2}$ , respectively, which are appropriate for the experimental sample.

The overall transmittance in the forward direction is ~90%, as high as that for the plastic substrate. Angular distribution measurements were conducted for both transmitted and reflected light from the nanopaper. A white light beam with 5 mm diameter was first normally incident on the nanopaper. A detector with an effective diameter of 1 cm was placed on the other side of the paper at a distance of 50 mm from the light spot on the paper, and at various angles from the incident beam. As shown in Fig. 3d, the transmitted light from the paper has a maximum at 0° (along the incident direction) and decreases slowly as the angle with the beam gets larger. The scattering effect is much more substantial compared to the plastic control sample. In order to measure the reflection angle distribution, a light beam with 5 mm diameter was incident at 45° from the surface normal of the nanopaper. The detector was placed in the same plane with the incident beam and surface normal. With a maximum at 45°, a significant amount of scattered light was also detected at different angles. As a comparison, the reflected light from a plastic slab shows a very sharp peak at 45°, which is very close to that of a mirror (Fig. 3c). Nanopaper with such a unique optical property can be applied

to optoelectronic devices, as demonstrated in a following section of this report.

To demonstrate the application of nanopaper substrates in optoelectronic devices, transparent conductors are deposited on nanopaper. Nanopaper is used as a substrate for the deposition of tin-doped indium oxide (ITO), carbon nanotubes (CNTs) or silver nanowires (AgNWs). These materials have previously been used on plastic or glass substrates as transparent electrodes.<sup>17–28</sup> There are a few advantages of using nanopaper as a replacement for these traditional substrates: (1) the 1D structure of nanopaper could partially solve the problem of mechanical instability of ITO on plastic or glass, as it could release the stress more effectively; (2) the porous structure allows excellent printing capability; (3) the high optical transmittance and large forward light scattering can bring new opportunities. For example, light scattering can decrease the reflection (glare) for enhanced visibility in bright environments and can increase the absorption in the active layer of solar cells to increase device performance. ITO films are deposited using radio frequency (RF) magnetron sputtering at 125 W with a gas mixture of 19 : 1 Ar : O<sub>2</sub> and a 2.5" target composed of 90% In<sub>2</sub>O<sub>3</sub> and 10% SnO<sub>2</sub> (Fig. S2†). Ink preparation and printing of CNTs or AgNWs follow a procedure described in our previous publications.<sup>4</sup> Briefly, an ink of CNTs or AgNWs is printed on a nanopaper substrate with a Meyer rod coating method and dried with an infrared light. Fig. 4a shows a transparent and conductive nanopaper with a 300 nm ITO film with a sheet resistance of 12 Ω sq<sup>-1</sup>. A mechanical tape test reveals that the binding between the conductive coating and nanopaper is strong. The sheet resistance is relatively low even after repeated bending of the conductive paper to very small radius (Fig. S3 and S4†). The overall performance of different transparent conductors on nanopaper is compared for ITO, AgNWs and CNTs (Fig. 4b). When the diffusive transmittance ( $T_d$ ) at 550 nm is used, a performance of 12 Ω sq<sup>-1</sup> and  $T_d = 65%$  is achieved for ITO, 200 Ω sq<sup>-1</sup> and  $T_d = 60%$  for CNT, and 25 Ω sq<sup>-1</sup> and  $T_d = 78%$  for AgNW. The performance is comparable with that on the plastic substrate.<sup>29</sup>

The transparent nanopaper substrates with large forward light scattering are excellent for solar cells. The light-scattering effect increases the light path length in the active layer, resulting in more light absorption in the active layer. Organic solar cells with regioregular poly(3-hexylthiophene) (P3HT, Rieke, EE-grade):[6,6]-phenyl-C<sub>61</sub>-butyric acid methyl ester (PCBM, Nano-C) as the light absorbing active layer were demonstrated with transparent and conductive nanopaper. Organic bulk heterojunction solar cells were prepared by spin-coating an aqueous solution of poly(3,4-ethylenedioxythiophene):poly(styrene sulfonate) (PEDOT:PSS, Clevis P VP AI 4083) onto ITO-coated nanopaper substrates. The porous nanopaper substrates were first fixed to glass substrate carriers using either transparent double-sided tape or the capillary forces of water. The PEDOT:PSS solution was spin-coated twice at 1200 rpm for 45 seconds with an intermediate drying step to provide a thick and smooth PEDOT:PSS layer. The PEDOT:PSS was dried at a temperature of 140 °C for 15 minutes before transferring into a nitrogen-filled glove box for further processing. Solutions of 1 : 1 (by weight) mixtures of P3HT and PCBM in *ortho*-dichlorobenzene (Aldrich) with a total solute concentration of 100 mg mL<sup>-1</sup> were spin-coated onto the PEDOT-coated substrates at a speed of 900 rpm for 45 seconds. After spin coating, the substrates were immediately placed in covered Petri dishes to dry slowly overnight. After drying, the samples were annealed at 110 °C for 10 minutes to promote an optimal bulk heterojunction microstructure. Metal electrodes consisting of 7 nm of Ca followed by 200 nm of Al were then thermally evaporated to form an electrical contact. Fig. 5a shows a picture of a finished device. All steps up to and including *I*-*V* testing were done inside a nitrogen glove box to prevent solar cell degradation.

Control samples made on standard glass substrates with patterned ITO, and with the same active layer solution, exhibited short-circuit currents ( $J_{sc}$ ) of 8.1 mA cm<sup>-2</sup>, open-circuit voltages ( $V_{oc}$ ) of 0.59 V, fill factors (FF) of 0.48 and an overall power conversion efficiency (PCE) of 2.3%. With an active layer solution concentration of 100 mg mL<sup>-1</sup>, these control samples are much thicker (~450 nm) than thickness-optimized control

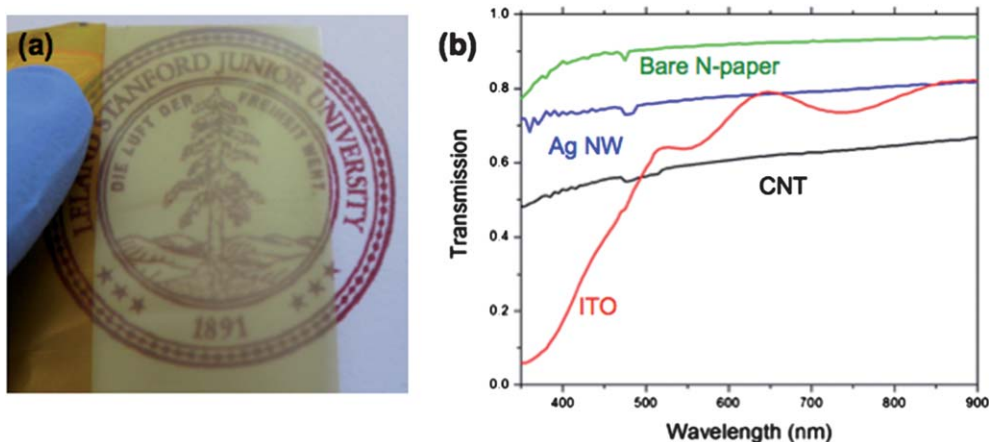


**Fig. 4** Transparent and conductive nanopaper. (a) Conductive nanopaper based on ITO with a performance of 12 Ω sq<sup>-1</sup> and 65% total transmittance at 550 nm. (b) Diffusive transmittance vs. wavelength for conductive nanopaper coated with CNT, ITO and AgNWs.

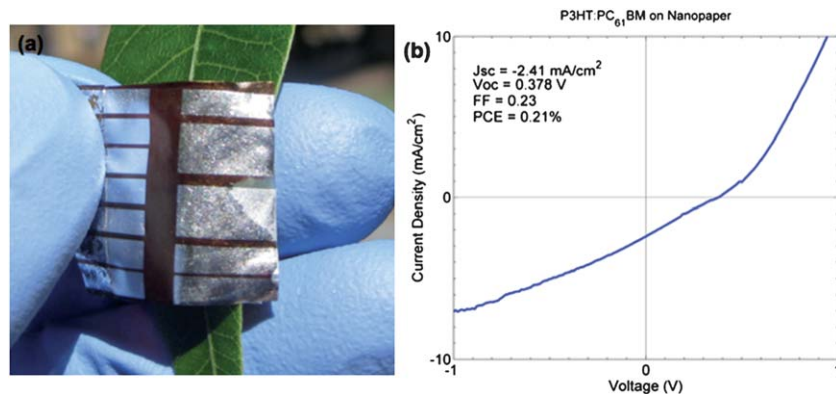


**Fig. 5** Printed solar cells on transparent and conductive nanopaper. (a) An organic solar cell on conductive nanopaper. (b) The  $I$ - $V$  curve of the organic solar cell shown in (a).

samples ( $\sim 220$  nm), which typically yield  $J_{SC}$  values of  $10 \text{ mA cm}^{-2}$ ,  $V_{OC}$  values of  $0.62 \text{ V}$ , fill factors near  $0.66$  and efficiencies of about  $4.0\%$ . While Fig. 5b shows poorer performance of these paper solar cells compared to the controls, they do show rectification and solar cell behavior. The low values of all performance parameters are possibly due to the higher sheet resistance of the ITO on the nanopaper substrate as compared to that on a traditional glass substrate. A fit to the linear portion of the dark  $I$ - $V$  curve in forward bias results in a measured series resistance of about  $100 \Omega \text{ cm}^2$ , nearly  $50$ – $100$  times higher than control samples. Other sample devices on nanopaper had larger currents (up to  $5.0 \text{ mA cm}^{-2}$ ) and efficiencies (up to  $0.40\%$  as a maximum) but often suffered from very poor rectification behavior likely due to shorts. The PEDOT layer on a perfectly smooth glass substrate is approximately  $25 \text{ nm}$  thick. When spin-coated onto a relatively rough surface (even one as smooth as nanopaper), the PEDOT layer will have thickness variation across the device that might result in small local shorting, decreasing the rectification capabilities of the device.

## Conclusion

A new type of flexible and transparent paper sheet made of cellulose nanofibrils has been prepared and used as a substrate for the optoelectronic device studies. Nanopaper shows a large difference between specular and diffusive transmittance. The large light scattering is helpful for solar cell applications. Solar cells with a power conversion efficiency of  $0.40\%$  were demonstrated. The cell efficiency could be further improved by modifying the nanopaper to maintain the surface smoothness during device fabrication. Transparent and conductive paper made from nanocellulose fibers will open up many opportunities in the fabrication of optoelectronic devices using renewable materials.

## Acknowledgements

This work was partially supported by King Abdullah University of Science and Technology Investigator Award KUS-I1-001-12. G.Z. acknowledges the financial support from the Agency for

Science, Technology and Research (A\*STAR), Singapore. M.E. and L.W. also acknowledge The Knut and Alice Wallenberg Research Foundation for financial support.

## References

- 1 E. Fortunato, N. Correia, P. Barquinha, L. Pereira, G. Goncalves and R. Martins, *IEEE Electron Device Lett.*, 2008, **29**, 988–990.
- 2 F. Eder, H. Klauk, M. Halik, U. Zschieschang, G. Schmid and C. Dehm, *Appl. Phys. Lett.*, 2004, **84**, 2673–2675.
- 3 M. C. Barr, J. A. Rowehl, R. R. Lunt, J. Xu, A. Wang, C. M. Boyce, S. G. Im, V. Bulovic and K. K. Gleason, *Adv. Mater.*, 2011, **23**, 3500.
- 4 L. Hu, J. W. Choi, Y. Yang, S. Jeong, F. La Mantia, L.-F. Cui and Y. Cui, *Proc. Natl. Acad. Sci. U. S. A.*, 2009, **106**, 21490–21494.
- 5 W. Lim, E. A. Douglas, S. H. Kim, D. P. Norton, S. J. Pearton, F. Ren, H. Shen and W. H. Chang, *Appl. Phys. Lett.*, 2009, **94**.
- 6 I. Siro and D. Plackett, *Cellulose*, 2010, **17**, 459–494.
- 7 H. Fukuzumi, T. Saito, T. Wata, Y. Kumamoto and A. Isogai, *Biomacromolecules*, 2009, **10**, 162–165.
- 8 M. Henriksson, L. A. Berglund, P. Isaksson, T. Lindstrom and T. Nishino, *Biomacromolecules*, 2008, **9**, 1579–1585.
- 9 M. Nogi, S. Iwamoto, A. N. Nakagaito and H. Yano, *Adv. Mater.*, 2009, **21**, 1595.
- 10 G. Nystrom, A. Mihranyan, A. Razaq, T. Lindstrom, L. Nyholm and M. Stromme, *J. Phys. Chem. B*, 2010, **114**, 4178–4182.
- 11 J. Wang, M. Liang, Y. Fang, T. Qiu, J. Zhang and L. Zhi, *Adv. Mater.*, 2012, **24**, 2874–2878.
- 12 X. Wang, L. Zhi and K. Mullen, *Nano Lett.*, 2007, **8**, 323–327.
- 13 H. C. v. d. Hulst, *Light Scattering by Small Particles*, Dover Publications, 1957.
- 14 L. Wågberg, G. Decher, M. Norgren, T. Lindstrom, M. Ankerfors and K. Axnaes, *Langmuir*, 2008, **24**, 784–795.
- 15 K. Klier, *J. Opt. Soc. Am.*, 1972, **62**, 882.
- 16 W. C. Chew, *Waves and Fields in Inhomogeneous Media*, IEEE Press, 1999.
- 17 P.-C. Chen, G. Shen, S. Sukcharoenchoke and C. Zhou, *Appl. Phys. Lett.*, 2009, **94**, 043113.

- 18 K. A. Sierros, D. S. Hecht, D. A. Banerjee, N. J. Morris, L. Hu, G. C. Irvin, R. S. Lee and D. R. Cairns, *Thin Solid Films*, 2010, **518**, 6977–6983.
- 19 S. De, T. M. Higgins, P. E. Lyons, E. M. Doherty, P. N. Nirmalraj, W. J. Blau, J. J. Boland and J. N. Coleman, *ACS Nano*, 2009, **3**, 1767–1774.
- 20 L. Hu, H. S. Kim, J.-Y. Lee, P. Peumans and Y. Cui, *ACS Nano*, 2010, **4**, 2955–2963.
- 21 Z. C. Wu, Z. H. Chen, X. Du, J. M. Logan, J. Sippel, M. Nikolou, K. Kamaras, J. R. Reynolds, D. B. Tanner, A. F. Hebard and A. G. Rinzler, *Science*, 2004, **305**, 1273–1276.
- 22 M. Zhang, S. L. Fang, A. A. Zakhidov, S. B. Lee, A. E. Aliev, C. D. Williams, K. R. Atkinson and R. H. Baughman, *Science*, 2005, **309**, 1215–1219.
- 23 L. Hu, D. S. Hecht and G. Gruner, *Nano Lett.*, 2004, **4**, 2513–2517.
- 24 Y. J. Lee and A. M. Belcher, *J. Mater. Chem.*, 2011, **21**, 1033–1039.
- 25 A. C. Dillon, *Chem. Rev.*, 2010, **110**, 6856–6872.
- 26 D. Azulai, T. Belenkova, H. Gilon, Z. Barkay and G. Markovich, *Nano Lett.*, 2009, **9**, 4246–4249.
- 27 X.-Y. Zeng, Q.-K. Zhang, R.-M. Yu and C.-Z. Lu, *Adv. Mater.*, 2010, **22**, 4484–4488.
- 28 D. Zhang, K. Ryu, X. Liu, E. Polikarpov, J. Ly, M. E. Tompson and C. Zhou, *Nano Lett.*, 2006, **6**, 1880–1886.
- 29 D. S. Hecht, L. Hu and G. Irvin, *Adv. Mater.*, 2011, **23**, 1482–1513.